The Astrophysical Journal, 710:828–835, 2010 February 10 doi:10.1088/0004-637X/710/1/828

SEARCH FOR VERY HIGH ENERGY GAMMA-RAY EMISSION FROM PULSAR-PULSAR WIND NEBULA SYSTEMS WITH THE MAGIC TELESCOPE

H. Anderhub[1], L. A. Antonelli[2], P. Antoranz[3], M. Backes[4], C. Baixeras[5], S. Balestra[3], J. A. Barrio[3], D. Bastieri[6], J. Becerra González[7], J. K. Becker[4], W. Bednarek[8], al K. Berger[8], E. Bernardini[9], A. Biland[1], R. K. Bock[6,10], G. Bonnoli[11], P. Bordas[12], D. Borla Tridon[10], V. Bosch-Ramon[12], D. Bose[3], I. Braun[1], T. Bretz[13], D. Britzger[10], M. Camara[3], E. Carmona[10], A. Carosi[2], P. Colin[10], S. Commichau[1], J. L. Contreras[3], J. Cortina[14], M. T. Costado[7,15], S. Covino[2], F. Dazzi[16,27], A. De Angelis[16], E. de Cea del Pozo[17], R. De los Reyes[3,28], B. De Lotto[16], M. De Maria[16], F. De Sabata[16], C. Delgado Mendez[7,29], A. Domínguez[18], D. Dominis Prester[19], D. Dorner[1], M. Doro[6], D. Elsaesser[13], M. Errando[14], D. Ferenc[20], E. Fernández[14], R. Firpo[14], M. V. Fonseca[3], L. Font[5], N. Galante[10], R. J. García López[7,15], M. Garczarczyk[14], M. Gaug[7], N. Godinovic[19], F. Goebel[10,30], D. Hadasch[5], A. Herrero[7,15], D. Hildebrand[1], D. Höhne-Mönch[13], J. Hose[10], D. Hrupec[19], C. C. Hsu[10], T. Jogler[10], S. Klepser[14], D. Kranich[1], A. La Barbera[2], A. Laille[20], E. Leonardo[11], E. Lindfors[21], S. Lombardi[6], F. Longo[16], M. López[6], E. Lorenz[1,10], P. Majumdar[9], G. Maneva[22], N. Mankuzhiyil[16], K. Mannheim[13], L. Maraschi[2], M. Mariotti[6], M. Martínez[14], D. Mazin[14], M. Meucci[11], J. M. Miranda[3], R. Mirzoyan[10], H. Miyamoto[10], J. Moldón[12], M. Moles[18], A. Moralejo[14], D. Nieto[3], K. Nilsson[21], J. Ninkovic[10], R. Orito[10], I. Oya[3], R. Paoletti[11], J. M. Paredes[12], M. Pasanen[21], D. Pascoli[6], F. Pauss[1], R. G. Pegna[11], M. A. Perez-Torres[18], M. Persic[16,23], L. Peruzzo[6], F. Prada[18], E. Prandini[6], N. Puchades[14], I. Puljak[19], I. Reichardt[14], W. Rhode[4], M. Ribó[12], J. Rico[14,24], M. Rissi[1], A. Robert[5], S. Rügamer[13], A. Saggion[6], T. Y. Saito[10], M. Salvati[2], M. Sánchez-Conde[18], K. Satalecka[9], V. Scalzotto[6], V. Scapin[16], T. Schweizer[10], M. Shayduk[10], S. N. Shore[25], A. Sierpowska-Bartosik[8], A. Sillanpää[21], J. Sitarek[8,10], D. Sobczynska[8], F. Spanier[13], S. Spiro[2], A. Stamerra[11], L. S. Stark[1], T. Suric[19], L. Takalo[21], F. Tavecchio[2], P. Temnikov[22], D. Tescaro[14], M. Teshima[10], D. F. Torres[17,24], N. Turini[11], H. Vankov[22], R. M. Wagner[10], V. Zabalza[12], F. Zandanel[18], R. Zanin[14], and J. Zapatero[5],

and

I. Cognard[26]

[1] ETH Zurich, CH-8093, Switzerland
[2] INAF National Institute for Astrophysics, I-00136 Rome, Italy
[3] Universidad Complutense, E-28040 Madrid, Spain; reyes@gae.ucm.es, miguel@gae.ucm.es
[4] Technische Universität Dortmund, D-44221 Dortmund, Germany
[5] Universitat Autònoma de Barcelona, E-08193 Bellaterra, Spain
[6] Università di Padova and INFN, I-35131 Padova, Italy
[7] Inst. de Astrofísica de Canarias, E-38200 La Laguna, Tenerife, Spain
[8] University of Łódź, PL-90236 Lodz, Poland; bednar@fizwe4.fic.uni.lodz.pl
[9] Deutsches Elektronen-Synchrotron (DESY), D-15738 Zeuthen, Germany
[10] Max-Planck-Institut für Physik, D-80805 München, Germany
[11] Università di Siena, and INFN Pisa, I-53100 Siena, Italy
[12] Universitat de Barcelona (ICC/IEEC), E-08028 Barcelona, Spain
[13] Universität Würzburg, D-97074 Würzburg, Germany
[14] IFAE, Edifici Cn., Campus UAB, E-08193 Bellaterra, Spain
[15] Depto. de Astrofísica, Universidad de La Laguna, E-38206 La Laguna, Tenerife, Spain
[16] Università di Udine, and INFN Trieste, I-33100 Udine, Italy
[17] Institut de Ciències de l'Espai (IEEC-CSIC), E-08193 Bellaterra, Spain
[18] Inst. de Astrofísica de Andalucía (CSIC), E-18080 Granada, Spain
[19] Rudjer Boskovic Institute, Bijenicka 54, HR-10000 Zagreb, Croatia
[20] University of California, Davis, CA-95616-8677, USA
[21] Tuorla Observatory, University of Turku, FI-21500 Piikkiö, Finland
[22] Inst. for Nucl. Research and Nucl. Energy, BG-1784 Sofia, Bulgaria
[23] INAF/Osservatorio Astronomico and INFN, I-34143 Trieste, Italy
[24] ICREA, E-08010 Barcelona, Spain
[25] Università di Pisa, and INFN Pisa, I-56126 Pisa, Italy
[26] LPC2E/CNRS, Orleans, France
Received 2009 August 24; accepted 2009 December 30; published 2010 January 22

ABSTRACT

The MAGIC collaboration has searched for high-energy gamma-ray emission of some of the most promising pulsar candidates above an energy threshold of 50 GeV, an energy not reachable up to now by other ground-based instruments. Neither pulsed nor steady gamma-ray emission has been observed at energies of 100 GeV from the classical radio pulsars PSR J0205+6449 and PSR J2229+6114 (and their nebulae 3C58 and Boomerang, respectively) and the millisecond pulsar PSR J0218+4232. Here, we present the flux upper limits for these sources and discuss their implications in the context of current model predictions.

Key words: gamma rays: stars – methods: observational – pulsars: individual (PSR J0205+6449, PSR J2229+6114, PSR J0218+4232) – telescopes

Online-only material: color figure

1. INTRODUCTION

More than 1800 pulsars have been discovered at radio frequencies, while at γ-ray energies the *Compton Gamma Ray Observatory* (*CGRO*) has detected only seven high-significance and three low-significance emitters of pulsed γ-rays up to energies of 5–10 GeV (Fierro 1995). *CGRO* observations showed evidence for a turndown in some of the studied pulsed spectra. Such spectral cutoffs were detected in Vela (Kanbach et al. 1994), and Geminga (Mayer-Hasselwander et al. 1994). For Crab (Nolan et al. 1993) and PSR B1951+32 (Srinivasan et al. 1997), there was only an indication of a possible cutoff in the GeV energy range. However, the other pulsars detected by *CGRO* showed no indication of a cutoff up to energies of 5–10 GeV (Fierro 1995; Thompson et al. 1999) because of insufficient sensitivity. On the other hand, no indication of pulsed emission in the energy band studied between 150 GeV and 50 TeV has been observed (Aharonian et al. 2007a; Albert et al. 2008b; Albert et al. 2007) by the previous generation of ground-based Imaging Air Cherenkov telescopes (IACT). Only recently, the energy gap from 5 to 150 GeV started to close as the MAGIC IACT has detected pulsed γ-emission from the Crab pulsar above 25 GeV (Aliu et al. 2008). The *Fermi* Observatory has recently detected pulsed emission from ∼46 γ-ray pulsars. These include a new pulsar in CTA 1 SNR (Abdo et al. 2008), the millisecond pulsar PSR J0030+0451 (Abdo et al. 2009c; Abdo et al. 2009e), and 23 of the EGRET sources, including the six high-confidence pulsars plus the three marginal detections, already confirmed (Abdo et al. 2009d). Among the *Fermi* pulsar population there are the three pulsars discussed in this paper, namely PSR J0205+6449, PSR J2229+6114 (Abdo et al. 2009a; Pellizzoni et al. 2009), and PSR J0218+4232 (Abdo et al. 2009c).

From a theoretical point of view, constraints on the pulsed high-energy emission of pulsars above tens of GeV are very important in order to decide which of the proposed models are really at work. Models in which gamma-rays are assumed to be produced in the inner regions of the pulsar magnetospheres (i.e., polar cap models; e.g., Harding 2005) have been recently constrained by the MAGIC detection of the pulsed emission from the Crab pulsar (Aliu et al. 2008). Other theoretical models (outer gap; e.g., Hirotani 2007) predict an inverse Compton component up to TeV energies, which can be constrained with MAGIC observations.

The models for steady emission from pulsar wind nebulae (PWNe) predict γ-ray fluxes which are typically within the sensitivities of the current Cherenkov telescopes above ∼100 GeV. That is the case of the PWNe around PSR J0205+6449 and PSR J2229+6114. The estimates based on the specific model for high-energy radiation from PWNe by Bednarek & Bartosik (2005) are of the order of ∼0.01–0.04 and ∼0.04–0.16 CU (Crab units or ratio of the steady Crab flux) above ∼200 GeV. In last years, VERITAS Collaboration reported upper limits on the level of 0.023 CU for PSR J0205+6449 and the detection (6.0σ) above 1 TeV of PSR J2229+6114 (Aliu et al. 2009). Also, the MILAGRO Collaboration reports intriguing detection (6.6σ) of a γ-ray source above 35 TeV coincident with PSR J2229+6114

Table 1
Top 12 List of the Best Pulsar Candidates from the ATNF Pulsar Catalogue (Manchester et al. 2005) Observable by MAGIC at Observation Zenith Angles Below 45°

Canonical Pulsars			Millisecond Pulsars		
Pulsar (PSR)	P (ms)	$\dot{E}/d^2$ ($\times 10^{38}$) (erg kpc^{-2} s^{-1})	Pulsar (PSR)	P (ms)	$\dot{E}/d^2$ ($\times 10^{34}$) (erg kpc^{-2} s^{-1})
B0531+21	33.1	1.2	B1957+20	1.6	6.8
J0205+6449	65.7	0.026	J0613−0200	3.1	5.8
J1833−1034	61.9	0.018	J0030+0451	4.9	3.8
J0633+1746	237.1	0.013	B1257+12	6.2	3.2
B1951+32	39.5	0.006	J0034−0534	1.9	3.1
J1930+1852	136.9	0.005	J1744−1134	4.1	2.3
B0656+14	384.9	0.005	J1024−0719	5.2	1.9
J1846−0258	325.7	0.003	J0751+1807	3.5	1.9
B1823−13	101.5	0.002	J1012+5307	5.3	1.7
J2229+6114	51.6	0.002	B1937+21	1.6	1.6
J1913+1011	35.9	0.001	J1843−1113	1.8	1.6
J1740+1000	154.1	0.001	**J0218+4232**	2.3	0.7

Note. The candidate list is divided between canonical (left) and millisecond (right) pulsars.

with the flux $(70.9 \pm 10.8) \times 10^{-17}$ TeV^{-1} cm^{-2} s^{-1} (Abdo et al. 2009b). These observations show some evidences that the emission can be extended.

We have selected the most promising pulsar candidates to be observed by MAGIC according to their spin-down flux ($\dot{E}/d^2$, spin-down luminosity divided by the distance) instead of using the predictions of a specific model. This selection criterion might also be valid for the best candidates of steady emission from the surrounding nebulae since the emission from the surroundings of the pulsar is directly related with the pulsar spin-down power. Table 1 shows the ordered list of the best candidates for MAGIC that follow this selection criterion with the additional constrain that the source must culminates at not too large zenith angles to assure the lowest possible energy threshold, which increases with the observation zenith angle. Within the canonical pulsar population, PSR J0205+6449 is, just after the Crab pulsar (PSR B0531+21), the most promising candidate followed by the EGRET detected pulsars Geminga (PSR J0633+1746), PSR B1951+32, and PSR J2229+6114. We included in our candidate list the millisecond pulsar, PSR J0218+4232 (ranking 12th in the table), which is of special interest because it is the first detected millisecond pulsar emitting pulsed γ-rays below 1 GeV (Kuiper et al. 2002). This list includes also PSR J0030+0451, recently detected by *Fermi* (Abdo et al. 2009c).

MAGIC uses two different trigger concepts. Up to late 2007, all data were taken with a standard trigger, providing a threshold of 50 GeV in a field of view (FOV) of about 1° radius around the candidate position (for ON/OFF observation mode), while a recently developed trigger logic, the so-called sumtrigger, allowed us to decrease the threshold down to 25 GeV but in a more restricted FOV (Rissi et al. 2008). This new trigger was used for the recent Crab pulsar detection (Aliu et al. 2008). Here, we present the analysis of data, which were recorded before 2008 with the standard trigger. The results with the standard trigger, with its higher threshold, could constrain models, which predict an energy cutoff in the spectrum below 50 GeV (polar cap) or around 100 GeV (outer gap) if the flux above that energy is high enough. Steady state (or unpulsed emission) from the host nebulae is expected to extend to higher energies and thus can be constrained with the high telescope sensitivity above ∼60 GeV.

[27] Supported by INFN Padova.
[28] Now at: Max-Planck-Institut für Kernphysik, P.O. Box 103980, D-69029 Heidelberg, Germany.
[29] Now at: Centro de Investigaciones Energéticas, Medioambientales y Tecnológicas (CIEMAT), Madrid, Spain.
[30] Deceased.

In the next sections, we will describe the observations and the data analysis of the target sources and the results for the search of very high energy (VHE) emission (pulsed and unpulsed) expected to be generated by the host nebulae (no pulsed or steady) and the pulsar (pulsed emission) as well as the specific analysis for the search of pulsed emission coming from the pulsar. This will be followed by a discussion about the implication of the results in the current theoretical models and by the conclusions.

2. OBSERVATIONS AND DATA ANALYSIS

2.1. Observations

Observations of the selected pulsars and the associated PWNe with the MAGIC Telescope have been carried out in 2005, 2006, and 2007 January. The single-dish MAGIC telescope (Lorenz 2004) is located at the Roque de los Muchachos observatory site (28°45′34″N, 17°5234W, 2200 m a.s.l.) on the Canary Island of La Palma. The telescope detects the Cherenkov light emitted by ultrarelativistic charged particles in air showers, which are produced by the interaction of γ-rays and charged cosmic rays with the Earth atmosphere. MAGIC consists of a tessellated primary reflector of 17 m of diameter supported by a lightweight frame made of carbon fiber reinforced plastic tubes. The small but unavoidable deformations of the support frame are corrected by an Active Mirror Control system, resulting in a point spread function of 0.°025. Shower images are recorded by a focal plane camera with a FOV of ∼3.°2 diameter. The camera comprises in its inner 2° FOV 394 photomultiplier (PMT) pixels of 0.°1 diameter and an outer zone comprising of 172 PMTs of 0.°2 diameter pixels. Once a trigger is issued, the signals from all the pixels of the camera, i.e., not only those containing the shower images but also those containing background light, are digitized by a 300 MHz Flash ADC (FADC) system[31] in a time window of 50 ns around the trigger time and written onto tape together with some auxiliary information such as the telescope pointing position during tracking and the event time from a rubidium clock synchronized via GPS to the US Naval observatory Master Clock Time (Washington, DC). The absolute time accuracy is 200 ns. Also, frequently, calibration events and pedestal events are recorded.

The observations were carried out in the so-called ON–OFF mode by using the standard trigger (Albert et al. 2008b). In this observation mode, one alternates observations pointing toward the source with others pointing to a nearby dark patch (without any known γ-ray source) in a sky area nearby the source. Since no dedicated OFF observations were carried out after observations of these sources, we blended the OFF data sample from a set of different contemporaneous observations in which no signal had been detected, covering the same zenith angle range and taken under similar technical (telescope performance) and atmospheric conditions. These conditions, together with the γ/hadron separation cuts, characterize the sensitivity of our analysis defined as the Crab flux fraction needed to detect 5σ in 50 hr.

2.2. Data Analysis

The data were analyzed with three different goals in mind:

1. At first, we searched for a possible summed γ-ray emission of the pulsar and PWN within the γ-ray point spread function of the telescope. For a possible signal, we searched for an excess at small angles in the *alpha*[32] distribution without any timing analysis constraints.
2. Second, we look for the presence of a periodic signal due to the pulsar while the photons from the PWN will contribute to the background.
3. In the third analysis, we searched for excess events coming from the pulsar surroundings making a scan of excess in alpha distribution in a FOV of 2° around the pulsar position.

The data are processed by the standard analysis program MARS (Bretz et al. 2005). First, data taken under bad atmospheric or technical conditions are discarded, as well as those events produced by background light flashes from bypassing cars, etc. The frequently recorded calibration data are used to convert the digitized signal (after pedestal subtraction) in each pixel to photons coming from the extensive air shower (EAS). To first order, the number of photons is a good measure of the incident γ-ray energy. Next, the shower images have to be filtered out of the background caused by the light of the night sky background (NSB) in the so-called core-boundary image cleaning algorithm. In this analysis, a core-boundary image cleaning level of 10–5 photoelectrons has been used, which yields the best telescope sensitivity in these observation periods. The cleaned images are then parameterized by the second-order moments of the light distribution in the image (Hillas 1985). The vast majority of the recorded images are due to hadron-induced air showers. In order to reject most of the hadronic background, a multidimensional events classification method has been used. The MAGIC collaboration has adopted as standard procedure, the Random Forest (RF) method, for the γ/hadron separation (Albert et al. 2008b). The method classifies the events according to the so-called *hadronness* parameter, which assigns to each event the probability of being a hadron. By applying a cut (as function of energy) in this parameter one can reduce the fraction of hadrons in the remaining sample while keeping a good efficiency for γ-ray events. The cuts have been optimized by training the RF on Crab data taken under similar conditions as the ON data analyzed[33] to get the best telescope sensitivity for each energy bin. The RF method is also used to estimate the energy of the primary particle that produced the detected air shower. The energy resolution of reconstructed events is 20% –30% depending on zenith angle of the observation and the gamma-ray energy. Finally, the direction of the shower is used to discriminate gamma-ray induced showers from the isotropic hadronic background. The analysis procedure normally used for the search of γ-ray emission from the source extracts the excess events in the source direction, subtracting in an *alpha* distribution the OFF data from the ON data at small *alpha* values after normalizing the OFF data to the ON data (at large *alpha* values). For our observations, we choose a cut in *alpha* of $\leqslant$ 10° (see, e.g., Figure 1). With these cuts, the resulting analysis has a sensitivity for a 5σ excess in the case of a minimum unpulsed flux of about 0.023 CU.[34] The significance of a signal is obtained through the Li & Ma expression (formula (17) of Li & Ma 1983). For pulsars, the sensitivity can be further enhanced exploiting the periodicity of the signal. If the phase diagram

[31] The 300 MHz FADC system was replaced in early 2007 by a faster one running at 2 GHz.

[32] Angle between the major axis of the shower image and the line that joins the center of gravity of the shower image with the source position in the camera plane (Hillas 1985).

[33] ON stands for an observation when the telescope is pointed to the source under study.

[34] The sensitivity could be improved in 2007 to a 0.014 CU limit in 50 hr of observation after introducing the new 2 GHz FADCs.

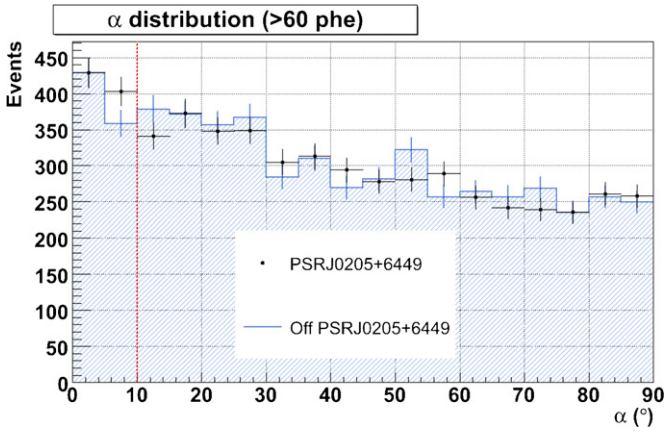

Figure 1. Alpha distribution of PSR J0205+6449 and 3C58 at energies $E > 220$ GeV ($E_{\rm th} \sim 320$ GeV). The ON and OFF data distributions are marked as the black points and the blue line, respectively. The red dotted line corresponds to the cut for the signal extraction ($\alpha < 10^\circ$).

(A color version of this figure is available in the online journal.)

contains only background events then no periodic structure is expected (see Section 2.3 on timing analysis). In case of no signal, we calculated integral flux upper limits by following the Rolke method (Rolke et al. 2005) for a 3σ confidence level.

As it has been confirmed by *Fermi* results (Abdo et al. 2009d), 19 out of 46 of the gamma-ray pulsars are associated with extended sources, like PSR J2229+6114 (Abdo et al. 2009b), associated with their PWN or the vicinity of the pulsar due to possible interaction between the PWN and the interstellar medium (ISM; Albert et al. 2008a) or from interactions between the PWN and the ISM due to the binary movement, as in the case of LSI +61 303 (Albert et al. 2008a). This last hypothesis is more often the case of millisecond pulsars. To look for emission in a wider region around the pulsar, we have to reconstruct from the shower parameters of each γ-ray event the possible origin in the sky plane. This is done through the so-called *disp*-algorithm (Domingo et al. 2006). It should be noted that for normal events we achieve a reconstruction error of $0.^\circ1$ for the origin of a γ-shower in the sky plane. The systematic pointing uncertainty due to unknown telescope deformation and tracking errors is estimated to be below $0.^\circ03$ (Albert et al. 2008b).

2.3. Timing Analysis

To search for pulsed VHE gamma-ray emission from the magnetosphere of a pulsar, we check whether the emission has a periodic behavior at the pulsar rotation frequency. The time of arrival (TOA) of each event is determined by a GPS–rubidium clock system. The first step is to convert the events arrival time measured at the observatory ($t_{\rm obs}$) to the pulsar reference frame. Neglecting second-order corrections, the nearest inertial reference frame to the pulsar rest frame is the solar system barycenter (SSB; Taylor & Weisberg 1989). The corrected arrival times are folded to the pulsar period, obtaining a phased data distribution or light curve, which is then tested against uniformity. Since the pulsar rotation period is independent of the wavelength of the emitted radiation, the pulsar ephemerides (frequency $\nu(T_0)$, frequency derivative $\dot{\nu}(T_0)$,...) at a reference time T_0 contemporaneous to the MAGIC observation period have been obtained from X-rays (*RXTE* satellite) and radio observations (Nançay radio telescope). Therefore, the effects of glitches and timing noise of the pulsar rotation are reduced and even eliminated in the pulsed emission analysis. The light curve of the pulsars studied here is characterized by a double-peaked structure; therefore, we have used a Pearson χ^2-test and a H-test (deJager et al. 1989) as statistical periodicity tests. Our timing analysis chain (López 2006) for short time difference between events was tested by analyzing optical data of the Crab pulsar recorded with the MAGIC central pixel (Lucarelli et al. 2008). Guided by the two main models of pulsar magnetosphere emission, the search for pulsed emission has been carried out in two energy intervals: the first at low energies, <300 GeV, and the second including all the events collected by the telescope in order to include the possible emission extended up to TeV energies. In both energy intervals, we have optimized the cut in the hadronness parameter for the γ/hadron separation by requiring that 80% of the γ-rays in Monte Carlo simulations survive the cuts.

3. RESULTS

3.1. PSR J0205+6449 and the PWN 3C58

Due to its similarities with the Crab Nebula, 3C58 was identified as a PWN twenty years before its pulsar was found, PSR J0205+6449, which initially was discovered by X-rays (Murray et al. 2002) and only afterward detected at radio frequencies (820 and 1375 MHz; Camilo et al. 2002). 3C58 was discovered by the Einstein Observatory and initially associated with the remnant of the supernova SN 1181 recorded in A.D. 1181 (Becker et al. 1982), thus implying an age of 820 yr. In recent years, this association has been rejected due to evidences of a significantly older spin-down age of 5400 yr and an expansion velocity of the nebula of $\sim$630 km s^{-1}. The distance to PSR J0205+6449 is 3.2 kpc. The pulsar has the second highest known spin-down power among all the members of the radio pulsar population in the Northern Hemisphere, $\sim$0.02 times the one of the Crab pulsar and $\sim$0.03 times the Vela one, and a magnetic field strength at the neutron star surface of the same order of magnitude ($B = 3.6 \times 10^{12}$ G) as Crab.

Observations of the PSR J0205+6449/3C58 complex were carried out by MAGIC between 2005 September–December (MJD = 53625–53707) at zenith angles ranging between 36°–45°. After rejecting all data taken during bad weather conditions or non-perfect detector response, 30 hr of data were left for analysis. The flux limit for a threshold of 320 GeV[35] to detect a 5σ unpulsed γ-ray signal corresponds to 0.028 CU. The results of the search for emission coming from the direction of PSR J0205+6449/3C58 are summarized in Table 2. No significant excess has been observed. The significance obtained, when integrating over the total energy range measured, is 1.0σ. The integral flux upper limit (99% c.l.) of PSR J0205+6449/3C58 for the complete energy range above 100 GeV is listed in Table 2. The upper limits for different energy bins (in GeV cm^{-2} s^{-1}) are shown in Figure 2 including also the Whipple flux upper limit for $E > 500$ GeV (Hall et al. 2001). The extension of the emission region of 3C58 is up to $6'$ at radio frequencies (Bietenholz 2006), which still corresponds to be point-like for the MAGIC angular resolution. A wider search in the pulsar surroundings has yielded no evidence of emission coming from the interaction of the PWN with the ISM at any energy.

Ephemeris for PSR J0205+6449 contemporaneous to the MAGIC observations were provided by the *RXTE* satellite S. Ransom (2006, private communication). Looking for an excess

[35] The above quoted threshold is, according to the convention in the γ-ray community, the peak of the recorded differential flux.

Table 2
Results for the Analysis of PSR J0205+6449/3C58, PSR J2229+6114/Boomerang Nebula, and PSR J0218+4232 for the Quoted Energy Bins E

Pulsar (PSR)	θ (°)	E (GeV)	$E_{\rm th}$ (GeV)	$N_{\rm exc}$	N_{bg}	S (σ)	$F_{3\sigma}$ ($\times 10^{-12}$) (cm^{-2} s^{-1})
J0205+6449/3C58	36–45	110–3e3	280	51	781 ± 34	1.0	7.7
J2229+6114/Boomerang	32–35	100–4e3	300	22	1230 ± 43	0.6	3.95
J0218+4232	14–32	70–5e3	140	49	7180 ± 100	0.4	31.7

Notes. The OFF background distribution is normalized to the ON distribution for *alpha* values > 30°. The number of excess events, i.e., from a potential signal, is $N_{\rm exc} = N_{On} - N_{bg}$ in the *alpha* range 0°–10°. Note that the threshold energy ($E_{\rm th}$) denotes the peak in the differential spectrum of a typical source with spectral index −2.6.

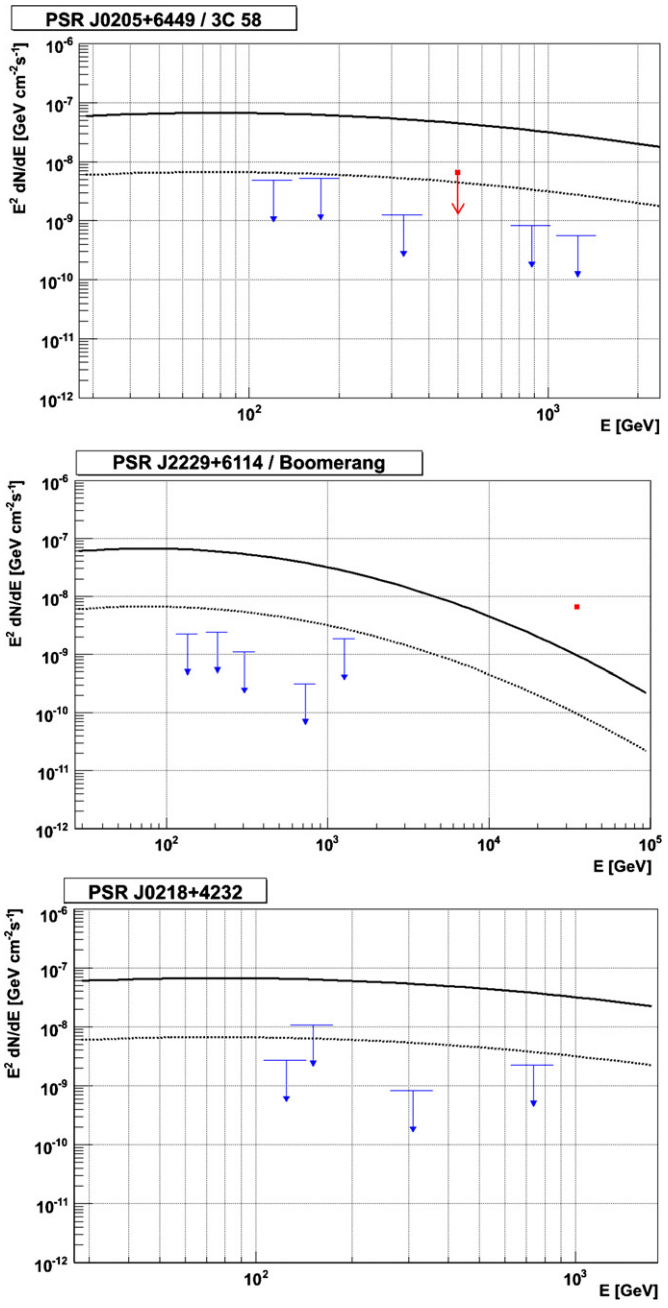

Figure 2. Unpulsed flux upper limits (99% c.l.) for the three pulsars and their corresponding nebulae from MAGIC observations (blue arrows): on top, 3C58 and PSR J0205+6449. The red filled square is the upper limit obtained from Whipple observations of 3C58 (Hall et al. 2001). In the middle, Boomerang and PSR J2229+6114. The detection of Boomerang nebula by Milagro (Abdo et al. 2009b) is marked as a filled red square. And at the bottom, PSR J0218+4232. The black lines denote different fractions of the Crab flux: the dashed line shows 0.1 CU and the solid line 1 CU.

Table 3
Results for the Pulsed Emission Analysis of PSR J0205+6449, PSR J0218+4232, and PSR J2229+6114 for the Energy Bins Below 300 GeV and the Total Observed Energy Bins

	E < 300 GeV		All E	
Pulsar (PSR)	Bg (%)	S (χ^2/H) (σ)	Bg (%)	S (χ^2/H) (σ)
J0205+6449	38	0.1/0.1	18	0.2/1.4
J2229+6114	32	0.8/0.2	20	0.6/0.8
J0218+4232	19	0.2/0.6	15	0.6/1.0

Notes. Bg is the ratio of the hadrons surviving the analysis cuts. S is the corresponding significance from χ^2/NDF and H statistical tests, respectively. NDF is defined as the number of degree of freedom.

of events in the phased data intervals corresponding to the peak positions at high energies, with respect to the off-pulsed region, we compute a significance of 0.2σ (see Table 3). Figure 3 shows the light curve of PSR J0205+6449 for low energies (E < 300 GeV). Since no pulsed emission has been detected, upper limits for the pulsed emission have been calculated requiring a confidence level of 99%. The upper limit to the pulsed emission of PSR J0205+6449 at this confidence level is $F_{\rm ul}^{3\sigma}$ ($E_{\rm th} = 280$ GeV) < 6.5×10^{-13} cm^{-2} s^{-1}, which includes γ-rays above 110 GeV.

3.2. PSR J2229+6114 and the Boomerang PWN

This pulsar was discovered in 2001 both in radio (Jodrell Bank Observatory) and in X-Rays (*Chandra* satellite; Halpern et al. 2001), inside the error box of the EGRET source 3EG J2227+6122, and within PWN G106.6+2.9. Its period (52 ms) and period derivative (7.83×10^{-14} s/s) imply a spin-down age of 10.5 kyr. The considered pulsar distance from X-rays measurements is around 3 kpc, while a considerable uncertainty remains depending on the radio dispersion measure (DM) model (Halpern et al. 2001). The surrounding nebula is called the Boomerang Nebula.

MAGIC observed this pulsar and its nebula, from 2005 August to December (MJD = 53584–53708) at zenith angles ranging between 32° and 38°. After excluding data taken under bad weather conditions or non-perfect detector response, we collected 10.5 hr of data suitable for the analysis. For 10.5 hr data and a threshold of 196 GeV, we expect a flux sensitivity of 0.03 CU. For the total range of accessible energies (E > 100 GeV), the significance of the excess events is 0.6σ. The corresponding upper limit (99% c.l.) is also listed in Table 2. The upper limits for different energy bins (in GeV cm^{-2} s^{-1}) are shown in Figure 2. A *disp*-analysis has revealed no emission in the surroundings of this source.

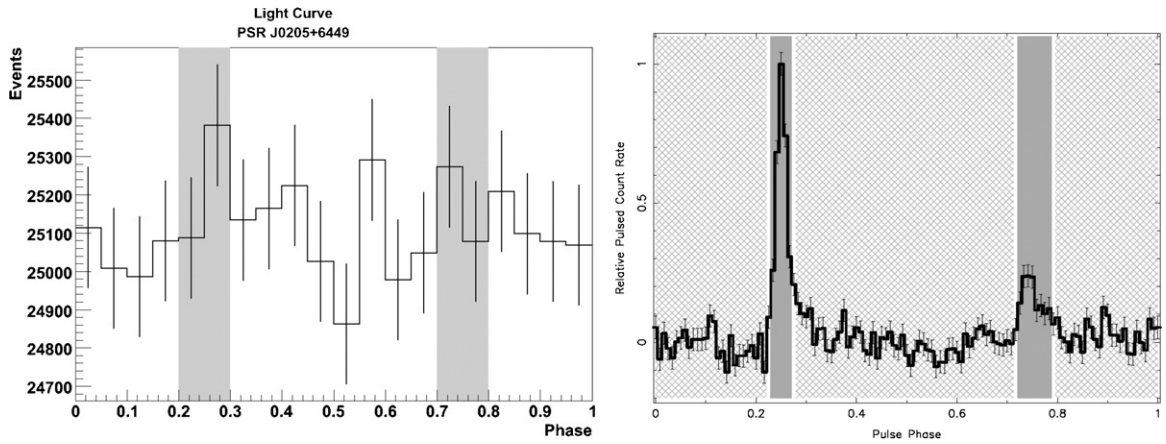

Figure 3. Left: light curve at PSR J0205+6449 for 80 GeV $< E <$ 300 GeV ($E_{\rm th} \sim$ 180 GeV). The shadowed area corresponds to the *RXTE* pulse peaks (Ransom et al. 2004; right). 0.1σ signal significance for the H-test.

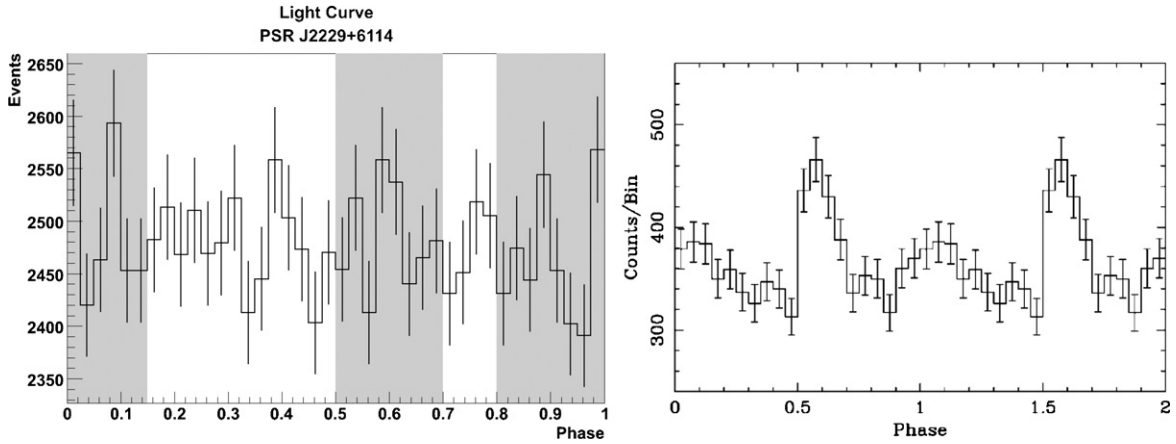

Figure 4. Left: light curve for PSR J2229+6114 at energies: 70 GeV $< E <$ 300 GeV, $E_{\rm th}$ ∼135 GeV, for the ephemerides frequency. The shadowed area corresponds to the ASCA GIS pulse peaks (0.8–10 keV; Halpern et al. 2001; phase diagram on the right). Signal significance ∼0.2 σ for H-test.

No significant pulsed signal from PSR J2229+6114 has been found for any of the considered energy ranges (see Table 3) using the closest ephemerides (Halpern et al. 2001) to the MAGIC observations. Since young pulsars often have glitches in a time period of 4 yr, the timing analysis of this source includes a scan in frequencies center in the frequency measured on 2001. No significant signal has been found either in this scan. Figure 4 shows the light curve of PSR J2229+6114 for low energies (70 GeV $<$ E $<$ 300 GeV). The upper limit for a possible pulsed emission has been calculated requiring a confidence level of 99%. The integral value for the total energy range is $F_{\rm ul}^{3\sigma}$ ($E_{\rm th}$ = 300 GeV) $< 2.6 \times 10^{-12}$ cm^{-2} s^{-1}, which includes γ-rays above 100 GeV.

3.3. PSR J0218+4232

Discovered at radio wavelengths (610 MHz; Navarro et al. 1995), the 2.3 ms pulsar PSR J0218+4232 belongs to a two-day orbital period binary system, at a distance of 5.7 kpc, with a low-mass (0.2 $M_{\odot}$) white dwarf companion. PSR J0218+4232 is one of the three known millisecond pulsars (together with PSR B1821−24 and PSR B1937+21) with a hard spectrum and high-luminosity emission in X-rays and the only one among them seen at γ-ray energies up to energies of 1 GeV before the launch of the *Fermi* Observatory. Above 1 GeV the EGRET detection is consistent, within the error box, with the nearby AGN 3C 66A (Kuiper et al. 2000). Although the pulsar phase diagram presents a large off-pulse contribution, no PWN emission has been observed from the direction of the source outside 1″ diameter from the pulsar position (Kuiper et al. 2002).

MAGIC observed PSR J0218+4232 at zenith angles between 14° and 32° during 2006 October and 2007 January (MJD = 54010–54115). After excluding data recorded under adverse weather conditions and non-perfect detector performance, 20 hr observation time were further analyzed. The analysis sensitivity for PSR J0218+4232 above 200 GeV is 0.033 CU. This sensitivity is slightly worse than the one of the two sources presented above, although the mean observation zenith angle is lower. The reason was hardware changes during the observation time that degraded the telescope performance. Figure 5 shows the phase diagram for the observed energy range for $E <$ 300 GeV. From the 0.4σ excess in the phase diagram using the period and peak positions at lower energies, we calculated the flux upper limit (for 99% CL) listed in Table 2. An analysis in three energy bins showed no signal in any bin. The corresponding upper limits (in GeV cm^{-2} s^{-1}) are shown in Figure 2. Previous observations at lower energies (radio and X-rays) have constrained the extension of a possible nebula around PSR J0218+4232 to be $<1''$ (Kuiper et al. 2002). Therefore, this source is considered to be point-like in the MAGIC energy domain. Although the millisecond pulsars are characterized to be very stable rotators, we used for our timing analysis ephemerides from the Nançay radio telescope contemporaneous to the MAGIC observation period. No emission has been

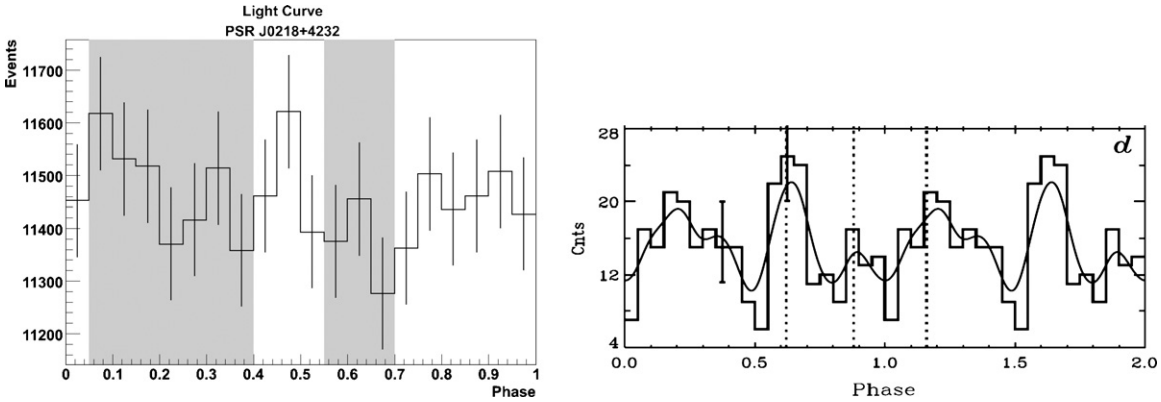

Figure 5. Left: light curve for PSR J0218+4232 for low energies (50 GeV $< E <$ 300 GeV, $E_{\rm th}$ ∼120 GeV). The shadowed area corresponds to the EGRET pulse peaks (Kuiper et al. 2002) in the phase diagram on the right. Signal significance (H-test) $\sim 0.6\sigma$.

detected for any assumption on the emission region and any analysis method; therefore, the corresponding upper limits to the pulsed emission have been calculated with a 99% confidence level. From the timing analysis of γ-rays above 70 GeV coming from PSR J0218+4232, we obtain an upper limit of $F_{\rm ul}^{3\sigma}$ ($E_{\rm th} =$ 140 GeV) $< 9.4 \times 10^{-12}$ cm^{-2} s^{-1}.

4. THE CONSEQUENCES OF THE PWNe UPPER LIMITS

The flux upper limits on the steady emission from the nebulae around two classical radio pulsars reported in this paper are close to the estimates based on the model for the TeV γ-ray emission from PWNe discussed by Bednarek & Bartosik (2005). In the case of the Boomerang nebula around PSR J2229+6114, the predicted flux above 200 GeV is ∼0.04 CU for the case of inverse Compton scattering of synchrotron and microwave background radiation. Bednarek & Bartosik (2005) consider also the model with significantly stronger low-energy background inside the nebula caused by the additional infrared component as expected in the case of the nebula around PSR 1706−44. In this case, the estimated flux above 200 GeV is ∼0.016 CU. Our observations definitively exclude the presence of such additional radiation field inside the Boomerang nebula. Moreover, there are some inconsistencies in the distance estimate to the PSR J2229+6114 which range between ∼3 kpc (used by Bednarek & Bartosik 2005) down to 0.8 kpc (Kothes et al. 2001). For the lower estimate of the distance, the flux estimated by Bednarek & Bartosik should be an order of magnitude larger. In this case, also the model with low soft radiation background inside the Boomerang nebula would be in contradiction with the MAGIC upper limit.

In the case of the nebula 3C58 around PSR J0205+6449, the flux estimated by Bednarek & Bartosik (2005) is lower between ∼0.8% with the low level of soft background inside the nebula up to ∼3.2% with the high level of soft background (additional infrared component). Therefore, in this case the upper limits reported in this paper cannot rule out the model.

Most recently, the MILAGRO collaboration has published a new list of TeV γ-ray sources at ∼35 TeV (Abdo et al. 2009b). One of them is coincident with the pulsar PSR J2229+6114, showing clear extension. If most of this emission comes from a relatively faint region around the PSR J2229+6114, the MILAGRO detection and the MAGIC upper limit at ∼1 TeV allows us to constrain the spectral shape at >100 GeV; the spectrum appears to be relatively flat with a spectral index $\leqslant 2$. This is very different than the Crab Nebula. This suggests that the acceleration and radiation processes inside the Boomerang nebula can differ significantly from those ones observed in the Crab Nebula.

5. CONCLUSIONS

Our search for VHE γ-ray emission from the pulsars PSR J0205+6449 and PSR J2229+6114 and the millisecond pulsar PSR J0218+4232 was negative. The MAGIC observations of these pulsars and their surroundings has yielded upper limits for the steady and the pulsed emission for energies above ∼70–100 GeV. This indicates that the possible pulsed TeV emission, as predicted by some theoretical models for the pulsed γ-ray emission (see, e.g., Hirotani 2007), seems to be below the MAGIC sensitivity in the explored energy range. In the case of MAGIC results for the millisecond pulsar PSR J0218+4232, the non-detection in the explored energy range above 70 GeV is consistent with some of the current models predictions, like our upper limits of the millisecond pulsar PSR J0218+4232 (Harding 2005). The rotational energy of the millisecond pulsar is much lower and, therefore, the spin-down energy is many orders of magnitude lower than in the class of young pulsars.

We also note that surprisingly some of the best candidate PWNe expected as a TeV γ-ray emitters have not been detected up to now (e.g., the nebulae around PSR B1951+32 (Albert et al. 2007) or PSR 1706−44 (Aharonian et al. 2007a)). On the other hand, it is quite interesting that some of the unidentified HESS TeV sources seem to be clearly related to PWNe (e.g., Aharonian et al. 2007b).

More sensitive and lower energy threshold Cherenkov telescopes are needed for the detection of these pulsars. The improved sensitivity of the future MAGIC stereo-system, formed by coincidence observations of MAGIC I and MAGIC II and the new trigger system used for the detection of the Crab pulsar above 25 GeV, should allow us to study these sources with a threshold around 25 GeV and will be thus crucial for the study of the Northern sky pulsars.

We thank the Instituto de Astrofisica de Canarias for the excellent working conditions at the Observatorio del Roque de los Muchachos in La Palma. The support of the German BMBF and MPG, the Italian INFN, and the Spanish MICINN is gratefully acknowledged. This work was also supported by ETH Research Grant TH 34/043, by the Polish MNiSzW Grant N N203 390834, and by the YIP of the Helmholtz Gemeinschaft.

We thank D. A. Smith and the Nançay Radio Observatory operated by the Paris Observatory (associated with the French

CNRS) for the ephemerides of PSR J0218+4232, and also S. M. Ransom (NRAO) for the ephemerides of PSR J0205+6449.

Facilities: MAGIC

REFERENCES

Abdo, A. A., et al. 2008, Science, 322, 1218
Abdo, A. A., et al. 2009a, ApJS, 183, 46
Abdo, A. A., et al. 2009b, ApJ, 700, L127
Abdo, A. A., et al. 2009c, ApJ, 699, 1171
Abdo, A. A., et al. 2009d, ApJ, submitted (arXiv:0910.1608)
Abdo, A. A., et al. 2009e, Science, 325, 848
Aharonian, F., et al. 2007a, A&A, 466, 543
Aharonian, F., et al. 2007b, A&A, 472, 489
Albert, J., et al. 2007, ApJ, 669, 1143
Albert, J., et al. 2008a, Science, 312, 1771
Albert, J., et al. 2008b, ApJ, 674, 1037
Aliu, E., et al. 2008, Science, 322, 1221
Aliu, E., et al. 2009, in Proc. TeV Particle Astrophysics 2009, Menlo Park, California, http://www-conf.slac.stanford.edu/tevpa09/Aliu090716.pdf
Becker, R. H., et al. 1982, ApJ, 255, 557
Bednarek, W., & Bartosik, M. 2005, J. Phys. G: Nucl. Part. Phys., 31, 1465
Bietenholz, M. F. 2006, ApJ, 645, 1180
Bretz, T., et al. 2005, in Proc. 29th ICRC, Vol. 4 (Pune), 315
Camilo, S., et al. 2002, ApJ, 571, L41
de Jager, O. C., et al. 1989, A&A, 221, 180
Domingo-Santamaria, E., et al. 2006, PhD thesis, Universitat Autonoma de Barcelona
Fierro, J. M. 1995, PhD thesis, Stanford University
Hall, T. A., et al. 2001, Proc. 27th ICRC, Vol. 6 (Hamburg), 2485
Halpern et al. 2001, ApJ, 552, L125
Harding, A. K. 2005, ApJ, 622, 531
Hillas, A. M. 1985, in Proc. 19th ICRC, Vol. 3, (La Jolla), 445
Hirotani, K. 2007, ApJ, 662, 1173
Kanbach, G., et al. 1994, A&A, 289, 855
Kothes, R., Uyaniker, B., & Pineault, S. 2001, ApJ, 560, 236
Kuiper, L., et al. 2000, A&A, 359, 615
Kuiper, L., et al. 2002, ApJ, 577, 917
Li, T., & Ma, Y. 1983, ApJ, 272, 317
Lorenz, E. 2004, New Astron. Rev., 48, 339
López, M. 2006, Ph.D. thesis, Univ. Complutense de Madrid
Lucarelli, F., et al. 2008, Nucl. Instrum. Methods Phys. Res. A, 589, 415
Manchester, R. N., et al. 2005, AJ, 129, 1993
Mayer-Hasselwander, H. A., et al. 1994, ApJ, 421, 276
Murray, S., et al. 2002, ApJ, 568, 226
Navarro, J., et al. 1995, ApJ, 455, L55
Nolan, P. L., et al. 1993, ApJ, 409, 697
Pellizzoni, A., et al. 2009, ApJ, 695, L115
Ransom, S., et al. 2004, in AIP Conf. Proc. 714, X-ray Timing 2003: Rossie and Beyond, ed. P. Kaaret, J. H. Swank, & F. K. Lamb (Melville, NY: AIP), 350
Rissi, M., et al. 2008, in Proc. 2008 Nuclear Science Symposium, Dresden
Rolke, W. A., et al. 2005, Nucl. Instrum. Methods Phys. Res. A, 551, 493
Srinivasan, R., et al. 1997, ApJ, 489, 170
Taylor, J. H., & Weisberg, J. M. 1989, ApJ, 345, 434
Thompson, D. J., et al. 1999, ApJ, 516, 297